Quantification of uncertainties in nonlinear vibrations of turbine blades with underplatform dampers

S. Bhatnagar, J. Yuan*, A. Fantetti, E. Denimal, L. Salles
Imperial College London, Department of Mechanical Engineering
South Kensington, SW7 2AZ, London,UK
e-mail: **jie.yuan@imperial.ac.uk**

Abstract
The high cycle fatigue life of turbine blades is negatively impacted by high frequency mechanical vibrations caused during operation. One method to mitigate this risk is to use underplatform dampers to dissipate energy from the system and reduce the vibration amplitude. Unfortunately, the state of the art models for such simulations are deterministic, although literature indicates that a large amount of uncertainty exists in measured contact parameters. This uncertainty in the contact parameters leads to significant variations in vibration response. This paper quantifies these uncertainties by considering the input parameters to be stochastic and generating uncertainty bands. A nonlinear solver based on Multi-Harmonic Balance method is used to propagate these uncertainties, and a surrogate model is implemented to increase the computational efficiency. Variance based sensitivity analysis is also performed to rank the importance of each uncertain parameter.

1 Introduction

The aerospace industry demands lighter and more efficient propulsion systems, thus driving the design of many components to their structural limits. During operation, a turbine blade experiences a combination of static and dynamic stresses [1]. The static stresses originate from thermal gradients, centrifugal loads and fluid pressure variation. On the other hand, dynamic stresses originate from mechanical and aero-dynamic vibration and have a negative impact on the high cycle fatigue (HCF) life [2]. Excessive stresses caused by significant vibrations can be dealt with by either moving the resonant frequency out of the operating range or by reducing the amplitude of vibration [3]. Whilst the former is theoretically achievable, it is not practically viable to avoid all resonant modes due to the wide distribution of such frequencies and hence the latter method is preferred. Reduced vibration amplitudes are achieved by removing energy from the system by using friction dampers [4, 5, 6]. These dampers work by exploiting the relative motion between them and the vibrating blades [7] leading to a local contact transition between stick and slip. In the slip condition, energy is dissipated at the contact surface, primarily as heat [8]. Optimizing the design of such dampers requires an accurate modelling approach to simulate the vibration amplitude response to a harmonic excitation. This also needs to be backed with experimental validation. Unfortunately, advances in validation methods of the numerical models have not kept up with the advances in the numerical models [9].

To obtain a better understanding of how to model friction dampers, and in particular underplatform dampers, a variety of studies have been conducted [10, 11]. Initially, simple models using single [12] and two degree of freedom [13] oscillators coupled with a type of Coulomb friction element (Jenkins Element [4]) were generated to investigate the dynamic response yielding partially analytic solutions. These systems were extended further by using complete FE models of the damper and bladed disks [8, 10, 11]. Underlying assumptions of the relative motion between the blades and damper proved difficult to validate suggesting the assumptions themselves were incorrect [8]. In order to remove these assumptions, models that calculated the damper motion directly were created [14, 15, 16]. Calculating damper motion required advanced 3D friction elements to model the in-plane tangential motion, normal load based separation and nonlinear contact forces

between the damper and blade. These advanced models are more accurate by better representing the damper-blade contact domain. The underplatform damper model developed by [9] can be classified as one of these advanced models.

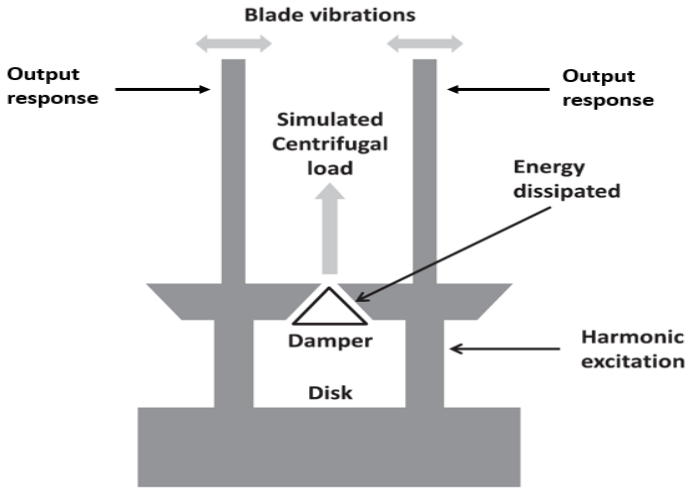

Figure 1: Underplatform Damper Rig Set-up [9]

In order to validate a greater fidelity underplatform model, Pesaresi et al. [9] have presented a dedicated UPD test rig based on a double beam configuration, shown in Figure fig:UPDrig. A 3D nonlinear model with an explicit FE damper design is the baseline of their analysis. The resulting underplatform damper study uses a nonlinear iterative solver, FORSE, to simulate the amplitude response of the model by calculating it at each excitation frequency in the studied frequency range. The output is represented by a type of frequency response function (FRF), accelerance (acceleration per newton ($m/s^2/N$)). The primary purpose of their study was to produce an accurate and replicable underplatform damper model [9]. The input contact parameters were assumed to be deterministic based on experimental testing. A deterministic variable is one which has the exact same, pre-determined value and presents no degree of uncertainty in its realization [17]. Unfortunately, the underplatform damper contact domain is highly dynamic due to variations in contact parameters over time caused by fretting wear [8]. As such, uncertainties are present in the amplitude response and frequency when this deterministic approach is utilised.

The aim of this investigation is to quantify the uncertainties in the output response of an underplatform damper model by taking the input parameters to be stochastic. The purpose of this procedure is to account for variations in the input parameters to better understand the design considerations needed for friction dampers. A further goal is to implement Polynomial Chaos Expansion (PCE), a surrogate modelling technique, to improve the computational efficiency of the numerical approach. The underplatform damper model presented by [9] is used as the test case.
Hence, this paper first presents a background into the modelling approach techniques. It is followed by the presentation of techniques to quantify the uncertainty in the system output are formalised. Finally, the results are presented and some trends are highlighted.

2 Reference model

A 3D nonlinear model with an explicit FE damper design is used as in this UQ study and is better descrobed in [9]. The FE models generated for the blades and damper consisted of quadratic hexahedral elements, made of steel. Each blade consists of 27486 elements and the damper consists of 3620 elements. As shown in Fig. fig:UPDrig, the sinusoidal excitation force is applied at bottom of a blade and displace-

ments are computed at the tip of the blades. The first two bending modes of the blades are studied here: an in-phase motion of the blades (mode 1) or an out-of-phase motion of the blades (mode 2) as illustrated in Figure fig:UPD$_modes.Inthepresenceofthedamper, theresonancefrequenciesare424.1Hzand440.3Hzrespectivelyatl

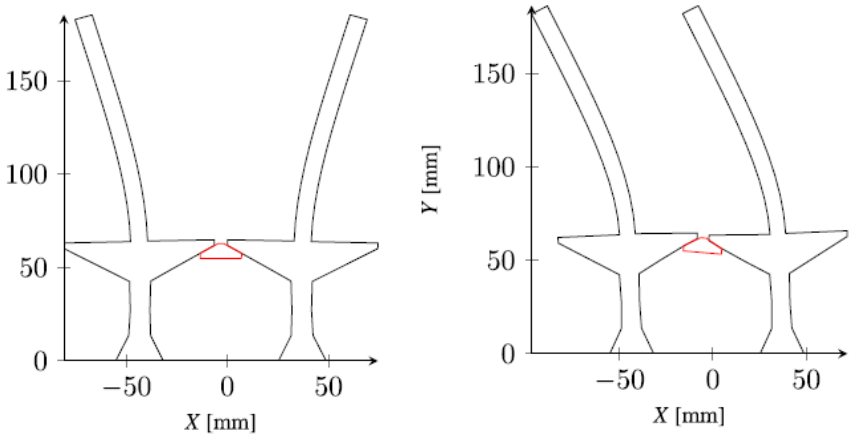

(a) (b)

Figure 2: (a) In-phase mode of the blades and (b) out-of-phase mode[9]

3 Modeling approach

A general nonlinear system of equations can be represented as follows:

$$\mathbf{M}\ddot{\mathbf{x}}(t) + \mathbf{C}\dot{\mathbf{x}}(t) + \mathbf{K}\mathbf{x}(t) + \mathbf{F}_{nl}(\dot{\mathbf{x}}(t), \mathbf{x}(t)) = \mathbf{F}_{ex}(t) \tag{1}$$

Where **M**, **C**, **K** are the mass, damping and stiffness matrices. $\mathbf{F}_{ex}$ is vector of external excitation forces and $\mathbf{F}_{nl}$ is the vector of nonlinear contact forces.

Time integration is the most rigorous approach to solve these set of equations [18]. However, it is computationally expensive and excessive when the steady-state response to harmonic excitation is the only study of interest. Consequently, the multi harmonic balance method (MHBM) [1, 19, 20] has been the most common approach to solve the nonlinear vibration system due to it being by far the most computationally efficient method [21]. MHBM solves the problem in the frequency domain due to the differential equations being represented as linear functions, making the system easier to solve. According to the MHBM, for each DOF in the system, the response can be expressed as a Fourier series truncated at the n^{th} harmonic, which generates a system of equations in the frequency domain.

A Newton-Raphson iterative solver is used to calculate the harmonic coefficients while the FRF matrix is obtained by calculating its exact value at a particular frequency point. A more detailed outline of the solving method can be found here [9]. The exact implementation of the nonlinear solver depends on the contact model used to describe the friction damping between the underplatform damper and blade root. The contact model used for the UPD rig is a 3D Jenkins element [19]. It is composed of two Jenkins element together with a normal spring. This allows both in-plane frictional forces and normal load based variations to be captured. The definition of each element is made through several contact parameters: the friction coefficient μ between the two surfaces, the contact tangential stiffness k_t and the normal stiffness k_n and a normal load N_0 representing the pre-load. The contact surface is discretised into several contact elements, and each element has its own contact parameters. This contact model allows for three different contact conditions: stick, slip and separation.

4 Uncertainty Sources in Contact Parameters

The primary source of uncertainty is in dynamics simulations of blades with dampers is the variability observed in experimentally measured contact parameters [22, 23, 24, 25]. During slip, the two rubbing surfaces undergo solid to solid contact which causes the surface roughness and stiffness to change. In addition, the change in damper geometry could lead to variations in blade coupling, resulting in the natural frequency to change. All of these factors lead to random variations in the values of the input parameters causing the amplitude response as well as the resonant frequency to become uncertain. It is important to quantify these uncertainties in order to account for these variations in the design of friction dampers [26]. Experimental testing has to be performed to estimate the variation of both the tangential contact stiffness k_t and the friction coefficient μ. In this study, k_t and μ were expressed as normally distributed parameters from experimental data presented in [23]:

- μ~N(0.9,0.05^2)
- k_t~N(60e6, 3e6^2)

5 Uncertainty propagation

Different strategies exist to propagate uncertainty in numerical models. Monte Carlo Simulations (MCS) remains the most robust method to do so [27], however convergence is slow and requires a large number of simulations making the approach unusable in practical applications. To cope with this issue, Polynomial Chaos Expansion (PCE) can be used to surrogate the dynamic behaviour of the structure. Once built, PCE models have negligible numerical cost and so can be exploited to perform different types of analysis as variance based sensitivity analysis [28, 29].

5.1 PCE model

The basis of PCE is outlined here, but detailed literature can be found here [29, 30, 31]. The principal concept of PCE is the ability to decompose a random process into independent deterministic and stochastic components. Generally, for a random process $\mathbf{A}$, that is a function of a random variable ξ and deterministic coefficients $\mathbf{x}$:

$$\mathbf{A}(\mathbf{x}, \xi) = \sum_{i=0}^{P} \mathbf{A}_i(\mathbf{x}) \Psi_i(\xi) \tag{2}$$

Where $\mathbf{A}_i(\mathbf{x})$ is the vector of deterministic coefficients and Ψ_i is the orthogonal polynomial basis mapping the coefficients to the random process. The choice of the polynomial basis is determined by the distribution of the random variable ξ and can be found directly from literature. For computational efficiency, the theoretically infinite sum of deterministic coefficients is truncated to P terms. The only unknown in Equation eqn:PCEmain is $\mathbf{A}_i(\mathbf{x})$. Both intrusive [32, 33] and non-intrusive (NIPCE) methods [17, 34] exist to solve for these coefficients but non-intrusive methods achieve this without the modification of the deterministic code that solves the nonlinear dynamic system. Hence, the non-intrusive regression method is employed here [29]. From a set of N evaluations of the system, a least-squares problem is solved to get the coefficients $\mathbf{A}_i(\mathbf{x})$. In the present study, a Latin Hypercube Sampling strategy is employed to generate the N input points. The construction of the PCE models are done with OpenTurns [31].

5.2 Variance based sensitivity analysis

Sobol analysis ranks the importance of the input parameters to the output response by measuring the change in the output's variance caused by a change in the input. The basis of the analysis is the ability to decompose the output variance into a sum of variances [28, 35] by creating linked sets of the input parameters.

$$V(output) = \sum_{i=1}^{n} V_i + \sum_{i \leq j < n}^{n} V_{ij} + ... + \sum_{i \leq n}^{n} V_{i...n} \tag{3}$$

In Equation eqn:sobol, $V(output)$ is the total variance of the output, V_i is the first order contribution of the ith stochastic parameter, V_{ij} is the second order contribution of interaction effects of the ith and jth parameter and n is the number of stochastic parameters. The first order sensitivity index for the ith parameter is calculated from Equation eqn:sobolindex:

$$S_{1,i} = \frac{V_i}{V(output)} \tag{4}$$

The variance decomposition from Equation eqn:sobol can be directly related to the PCE decomposition eqn:PCEmain[29], and so the Sobol indices can be directly determined from the PCE coefficients without any additional simulation [31].

6 Results

6.1 Nonlinear Vibration response

As explained previously, the first two bending modes of the structure are considered, which are the in-phase (mode 1) and out-of-phase (mode 2) motion of the two blades. Figure fig:amp$_c onditions(a,b) shows receptances for diff$ $f). It can be seen that for low shaker force amplitudes, both modes are sticking, resulting in low damping. Increasing t$

6.2 Uncertainty Quantification

In this section, the uncertainty associated to the contact parameters is propagated using the PCE method explained previously. The set of input points used to construct the PCE is generated with a LHS of 100 combinations of contact parameter values. For each of those combinations, the FRFs for both in-phase and out-of-phase modes were computed at different excitation amplitudes. Results for the 17N excitation loading are presented in Figure fig:rawData.

Since the FRFs are strongly non linear, the PCE meta-model cannot be constructed as a function of the frequency (in fact, for some frequency values there are more receptance solutions). To avoid this problem, the deterministic parameter used is the phase [34]. Figures fig:freqMap and fig:phaseMap show how the frequency is mapped to the phase. It should be noted that the phase decreases cyclically for each mode. Once each FRF is decomposed into a phase frequency response and a phase amplitude response, two PCE meta-models are built for each mode and each phase value: one for the amplitude and one for the frequency.

Such PCE meta-modes can be exploited with an almost null numerical cost to generate the statistical distribution of the system response. Uncertainty bands obtained from those meta-models are shown in Figure fig:UQ$_b ands for the two modes with an excitation amplitude of 17\ N. For the receptance, the uncertainty is negligi$
$-\pi/2$ radians). The uncertainty in the frequency vector is also negligible at the extreme phase values, while it increases around resonance, as shown in Figure fig:UQ$_b ands(b). The same trends are present for the second mode, shown$

6.3 Sobol indices

First order Sobol indices were also calculated directly from the PCE model to get insights into the influence of each contact parameter on the system dynamics. The contact conditions for the damper-blade nodes (as a percentage) were used in combination with Sobol indices to help explain the behaviour. Results are displayed in Figure fig:Solbol.

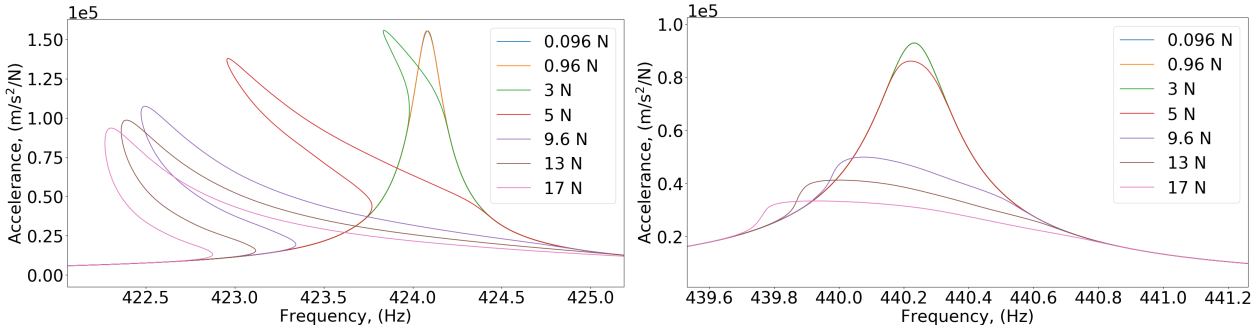

(a) Amplitude response in phase peak

(b) Amplitude response out of phase peak

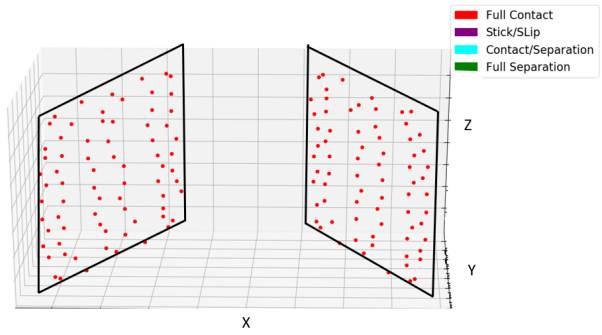

(c) Amplitude = 0.096 N, mode 1

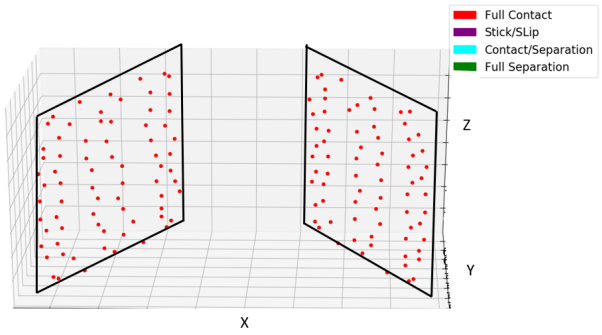

(d) Amplitude = 0.096 N, mode 2

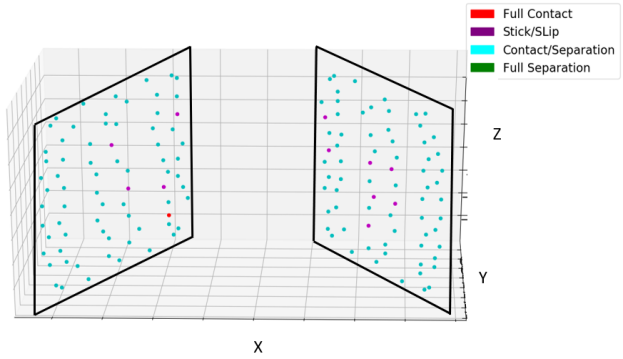

(e) Amplitude = 17 N, mode 1

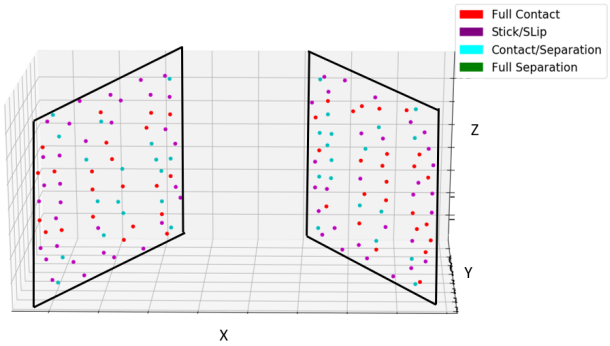

(f) Amplitude = 17 N, mode 2

Figure 3: Forced response and contact conditions for shaker force amplitude sensitivity analysis

For the accelerance, it is evident that when the system has no slip, k_t fully determines the system response as the first order Soblol index of k_t is equal to 1, while μ has no impact. This can be seen in Figures fig:PCE$_s obol_a mp1 and fig : PCE_s obol_a mp2. However, upon any percentage of slip, this pattern flips and \mu$ solely determines the system response as its first order Sobol index becomes equal to 1. This pattern is expected as during slip, the amplitude response is determined by the amount of damping and the amount of damping is determined by friction. In the stick case, there is no sliding and so μ is not relevant in determining the output response.

On the contrary, the Sobol indices for the frequency do not have such a clear pattern, as shown by Figures fig:PCE$_s obol_f req1 and fig : PCE_s obol_f req2. In general, for both modes, the tangential stiffness primarily determi
Around the ends of each plot, k_t determines the output completely. This is expected with the system being in the stick condition as confirmed by the stick percentage. For the second mode, from a phase of -1 to 1 radians, the contact conditions do not vary significantly indicating the Sobol indices should follow a similar pattern. Rather surprisingly, there is a local minimum in the μ index and a local maximum in the k_t index for both

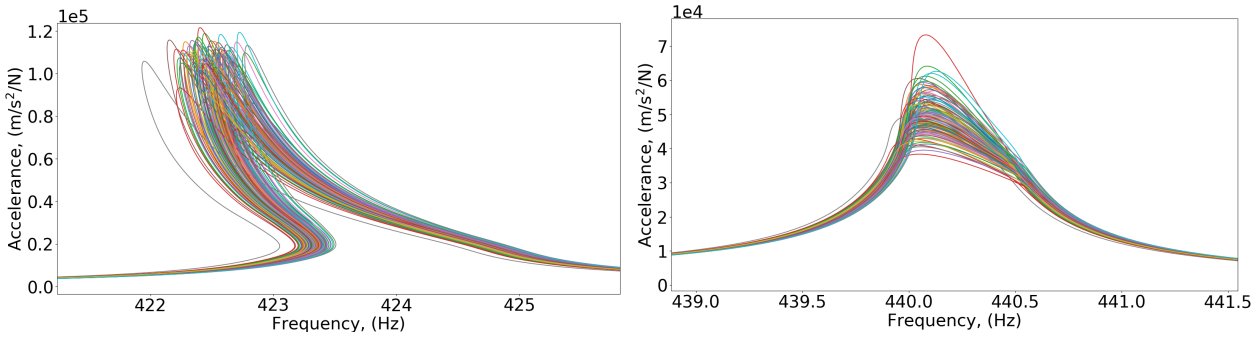

(a) Mode 1 - Raw data

(b) Mode 2 - Raw data

Figure 4: 100 LHS simulations run through FORSE, μ~N(0.6,0.05^2) and k_t~N(60e6, 3e6^2)

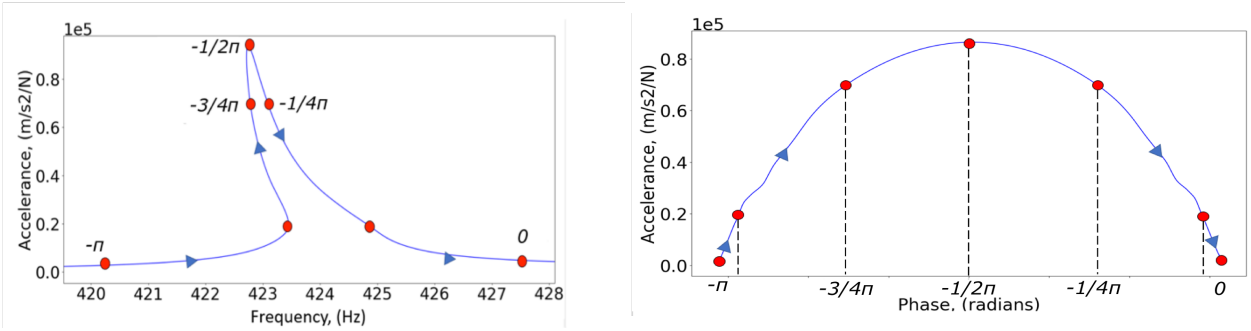

(a) Mode 1 with phase equivalent points

(b) Mode 1 with frequency equivalent points

Figure 5: Frequency and phase equivalency

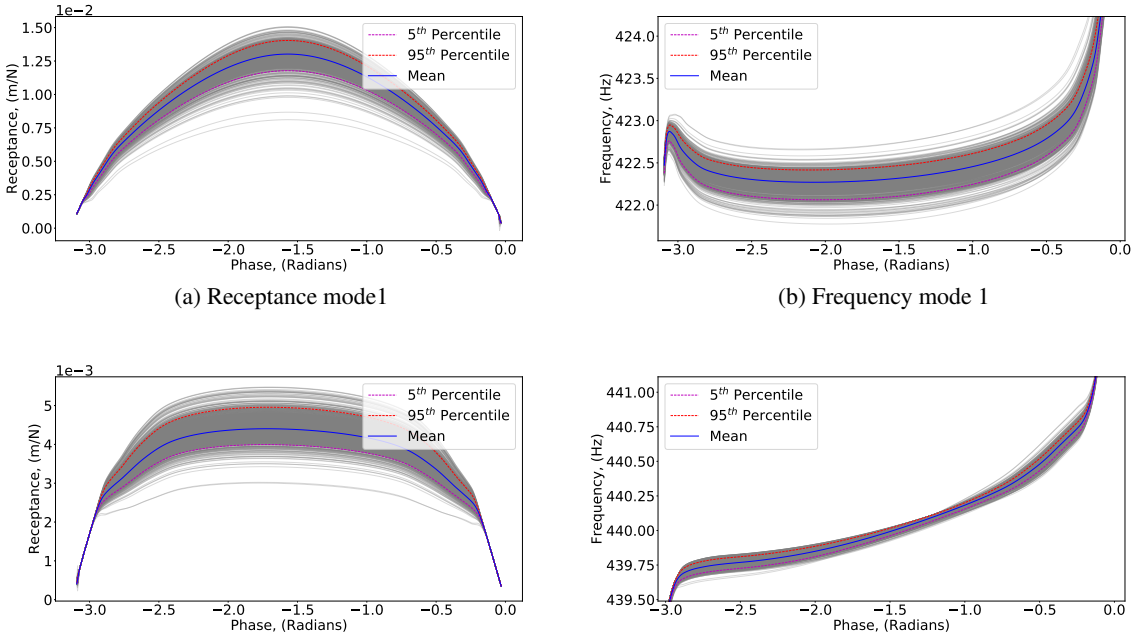

(a) Receptance mode1

(b) Frequency mode 1

(c) Receptance mode2

(d) Frequency mode 2

Figure 6: Uncertainty bands based on PCE model

modes around resonance, shown in Figures fig:PCE$_sobol_freq1 and fig : PCE_sobol_freq2. The reason for this behaviour$

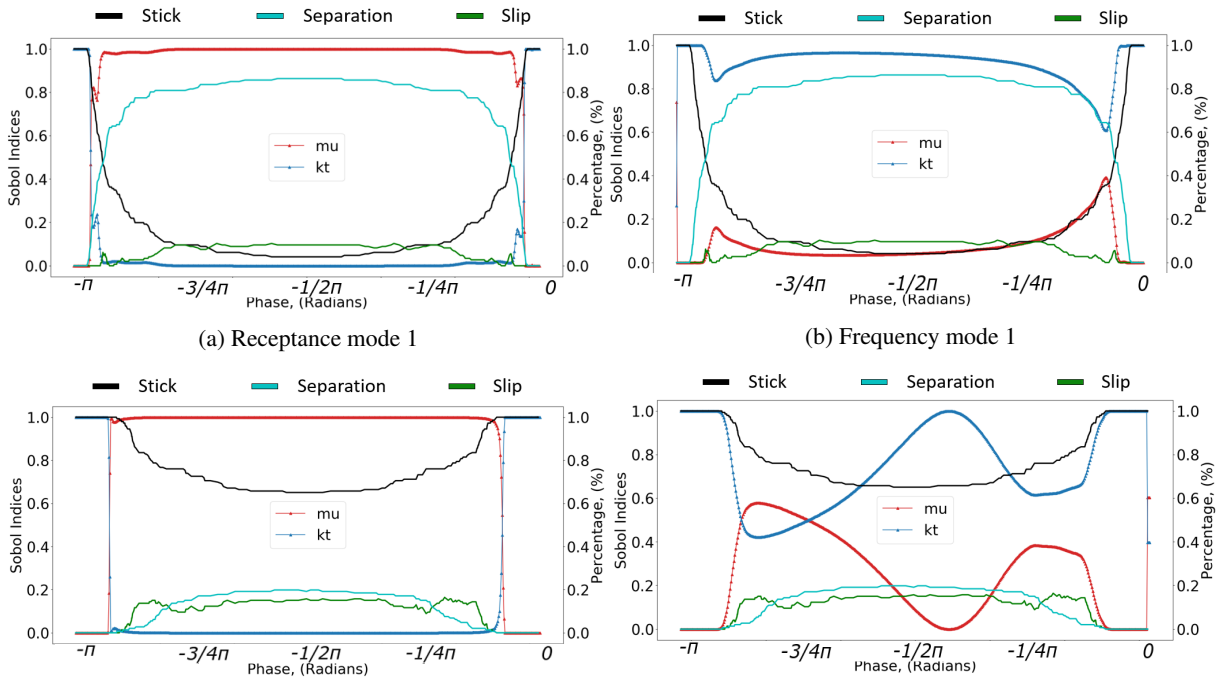

(a) Receptance mode 1

(b) Frequency mode 1

(c) Receptance mode 2

(d) Frequency mode 2

Figure 7: Sobol indices for accelerance, frequency with contact conditions superimposed

and a varying μ (here not shown). The simulations showed that for the 0.2 radians case, the frequency remains constant and only the amplitude varies as μ was changed, which explains these results.

Combining the Sobol analysis with the uncertainty bands, it is evident that uncertainty in accelerance is present only in the slip region and as the output in this region is determined by variations in μ only, it can be concluded that variations in μ determine the uncertainty in accelerance. For the frequency, uncertainties are present throughout. k_t primarily determines the amount of uncertainty but local peaks in slip increase the contribution of μ. The uncertainty in resonant frequency is solely determined by variations in k_t with μ altering the resonance amplitude only.

7 Conclusion

A method to quantify the uncertainties in the nonlinear response of an underplatform damper model has been successfully developed. The method is based on the generation of PCE meta-models, which make it possible to have a large sample size thus improving statistical accuracy as well as offering a significant reduction in computation time.

Uncertainty bands in the frequency response functions (FRFs) were obtained from these meta-models. Also a Sobol analysis was performed to rank the sensitivity of the FRFs on the different contact parameteres. From this analysis it was found that, for the accelerance, uncertainties only exist while the system is slipping. In this region, the extent of uncertainty is determined by variations in μ. Under the stick condition, μ has no impact and k_t should control the accelerance amplitude. On the contrary, in the case of frequency, uncertainties are determined mainly by variations in k_t, although trends are not directly related to the slipping conditions.

With regards to optimisation of damper design, the proposed uncertainty quantification method is useful since it provides bands in the output responses. With this information, damper design criteria can be updated to better inform the design decisions. In addition, the Sobol analysis allows the prioritisation of design decisions based on their impact on the output. Finally, the implementation of the PCE model makes the process computationally very efficient allowing wider underplatform damper studies to be performed with fewer computational resources. In order to have complete confidence in the statistical bands generated, an

experimental validation of the approach will be performed with future work.

Acknowledgements

The authors would like to acknowledge the support of Rolls-Royce plc through the Vibration University Technology Centre (UTC) at Imperial College London, UK

References

[1] M. Krack, L. Salles, and F. Thouverez, "Vibration prediction of bladed disks coupled by friction joints," *Archives of Computational Methods in Engineering*, vol. 24, no. 3, pp. 589–636, 2017.

[2] J. Yuan, F. Scarpa, G. Allegri, B. Titurus, S. Patsias, and R. Rajasekaran, "Efficient computational techniques for mistuning analysis of bladed discs: a review," *Mechanical Systems and Signal Processing*, vol. 87, pp. 71–90, 2017.

[3] J. H. Griffin, "A review of friction damping of turbine blade vibration," *International Journal of Turbo and Jet Engines*, vol. 7, no. 3-4, pp. 297–308, 1990.

[4] L. Gaul and R. Nitsche, "The role of friction in mechanical joints," *Applied Mechanics Reviews*, vol. 54, no. 2, pp. 93–106, 2001.

[5] B. Feeny, A. Guran, N. Hinrichs, and K. Popp, "A historical review on dry friction and stick-slip phenomena," *Applied Mechanics Reviews*, vol. 51, no. 5, pp. 321–341, 1998.

[6] A. Fantetti, C. Gastaldi, and B. T, "Modelling and testing flexible friction dampers : challenges and peculiarities," *Experimental Techniques*, 2018.

[7] K. Y. Sanliturk, D. J. Ewins, R. Elliott, and J. S. Green, "Friction damper optimisation: simulation of rainbow tests," in *ASME 1999 International Gas Turbine and Aeroengine Congress and Exhibition*. American Society of Mechanical Engineers, 1999, pp. V004T03A038–V004T03A038.

[8] K. Y. Sanliturk, D. J. Ewins, and A. B. Stanbridge, "Underplatform dampers for turbine blades: theoretical modeling, analysis, and comparison with experimental data," *Journal of Engineering for Gas Turbines and Power*, vol. 123, no. 4, pp. 919–929, 2001.

[9] L. Pesaresi, L. Salles, A. Jones, J. Green, and C. Schwingshackl, "Modelling the nonlinear behaviour of an underplatform damper test rig for turbine applications," *Mechanical Systems and Signal Processing*, vol. 85, pp. 662–679, 2017.

[10] G. Csaba, "Forced response analysis in time and frequency domains of a tuned bladed disk with friction dampers," *Journal of Sound and Vibration*, vol. 214, no. 3, pp. 395–412, 1998.

[11] B. Yang and C. Menq, "Characterization of contact kinematics and application to the design of wedge dampers in turbomachinery blading: Part i—stick-slip contact kinematics," in *ASME 1997 International Gas Turbine and Aeroengine Congress and Exhibition*. American Society of Mechanical Engineers, 1997, pp. V004T14A007–V004T14A007.

[12] T. Cameron, J. Griffin, R. Kielb, and T. Hoosac, "An integrated approach for friction damper design," *Journal of Vibration and Acoustics*, vol. 112, no. 2, pp. 175–182, 1990.

[13] G. C. Yeh, "Forced vibrations of a two-degree-of-freedom system with combined coulomb and viscous damping," *The Journal of the Acoustical Society of America*, vol. 39, no. 1, pp. 14–24, 1966.

[14] S. Zucca, C. M. Firrone, and M. Gola, "Modeling underplatform dampers for turbine blades: a refined approach in the frequency domain," *Journal of Vibration and Control*, vol. 19, no. 7, pp. 1087–1102, 2013.

[15] E. Petrov and D. Ewins, "Advanced modeling of underplatform friction dampers for analysis of bladed disk vibration," *Journal of Turbomachinery*, vol. 129, no. 1, pp. 143–150, 2007.

[16] C. Gastaldi, A. Fantetti, and B. T, "Forced response prediction of turbine blades with flexible dampers: The impact of engineering modelling choices," *Applied Sciences*, 2017.

[17] T. Roncen, J.-J. Sinou, and J. Lambelin, "Non-linear vibrations of a beam with non-ideal boundary conditions and uncertainties–modeling, numerical simulations and experiments," *Mechanical Systems and Signal Processing*, vol. 110, pp. 165–179, 2018.

[18] K. Park, "An improved stiffly stable method for direct integration of nonlinear structural dynamic equations," *Journal of Applied Mechanics*, vol. 42, no. 2, pp. 464–470, 1975.

[19] E. Petrov and D. Ewins, "Analytical formulation of friction interface elements for analysis of nonlinear multi-harmonic vibrations of bladed disks," *Journal of Turbomachinery*, vol. 125, no. 2, pp. 364–371, 2003.

[20] E. Petrov, "A high-accuracy model reduction for analysis of nonlinear vibrations in structures with contact interfaces," *Journal of Engineering for Gas Turbines and Power*, vol. 133, no. 10, p. 102503, 2011.

[21] T. Cameron and J. Griffin, "An alternating frequency/time domain method for calculating the steady-state response of nonlinear dynamic systems," *Journal of applied mechanics*, vol. 56, no. 1, pp. 149–154, 1989.

[22] A. Fantetti and C. Schwingshackl, "Effect of friction on the structural dynamics of built-ip structures: An experimental study," *Proceedings of ASME Turbo Expo 2020 Turbomachinery Technical Conference and Exposition*, 2020.

[23] A. Fantetti, L. Tamatam, M. Volvert, I. Lawal, L. Liu, L. Salles, M. Brake, C. Schwingshackl, and D. Nowell, "The impact of fretting wear on structural dynamics: Experiment and simulation," *Tribology International*, vol. 138, pp. 111–124, 2019.

[24] L. Pesaresi, A. Fantetti, F. Cegla, L. Salles, and C. Schwingshackl, "On the use of ultrasound waves to monitor the local dynamics of friction joints," *Experimental Mechanics*, vol. 60, pp. 129–141, 2020.

[25] A. Fantetti, C. Pennisi, D. Botto, S. Zucca, and C. Schwingshackl, "Comparison of contact parameters measured with two different friction rigs for nonlinear dynamic analysis," *International Conference on Noise and Vibration Engineering*, 2020.

[26] C. Gastaldi, B. T, and G. M, "The effect of surface finish on the proper functioning of underplatform dampers," *Journal of Vibration and Acoustics*, 2020.

[27] J. Yuan, G. Allegri, F. Scarpa, R. Rajasekaran, and S. Patsias, "Probabilistic dynamics of mistuned bladed disc systems using subset simulation," *Journal of Sound and Vibration*, vol. 350, pp. 185–198, 2015.

[28] B. Iooss and P. Lemaître, "A review on global sensitivity analysis methods," in *Uncertainty management in simulation-optimization of complex systems*. Springer, 2015, pp. 101–122.

[29] B. Sudret, "Global sensitivity analysis using polynomial chaos expansions," *Reliability engineering & system safety*, vol. 93, no. 7, pp. 964–979, 2008.

[30] T. Crestaux, O. Le Maıtre, and J.-M. Martinez, "Polynomial chaos expansion for sensitivity analysis," *Reliability Engineering & System Safety*, vol. 94, no. 7, pp. 1161–1172, 2009.

[31] B. I. A.-L. P. Michaël Baudin, Anne Dutfoy, "Openturns - an industrial software for uncertainty quantification in simulation," 2015.

[32] J. Didier, J.-J. Sinou, and B. Faverjon, "Nonlinear vibrations of a mechanical system with non-regular nonlinearities and uncertainties," *Communications in Nonlinear Science and Numerical Simulation*, vol. 18, no. 11, pp. 3250–3270, 2013.

[33] J.-J. Sinou, J. Didier, and B. Faverjon, "Stochastic non-linear response of a flexible rotor with local non-linearities," *International Journal of Non-Linear Mechanics*, vol. 74, pp. 92–99, 2015.

[34] E. Sarrouy, "Phase driven study for stochastic linear multi-dofs dynamic response," *Mechanical Systems and Signal Processing*, vol. 129, pp. 717–740, 2019.

[35] W. Xie, Y. Yang, S. Meng, T. Peng, J. Yuan, F. Scarpa, C. Xu, and H. Jin, "Probabilistic reliability analysis of carbon/carbon composite nozzle cones with uncertain parameters," *Journal of Spacecraft and Rockets*, vol. 56, no. 6, pp. 1765–1774, 2019.